

## In-Plane Dissipation Maxima and Vortex-Line Distortions in the Resistive Transitions of Oxygen-Doped $\text{Bi}_2\text{Sr}_2\text{CaCu}_2\text{O}_{8+\delta}$ Single Crystals

J. W. P. Hsu,<sup>(a)</sup> D. B. Mitzi,<sup>(b)</sup> and A. Kapitulnik

*Department of Applied Physics, Stanford University, Stanford, California 94305*

Mark Lee

*NEC Research Institute, Princeton, New Jersey 08540*

(Received 5 June 1991)

Measurements of the in-plane resistive transition of  $\text{Bi}_2\text{Sr}_2\text{CaCu}_2\text{O}_{8+\delta}$  single crystals in perpendicular magnetic fields reveal that in oxygen-reduced samples a giant resistance maximum evolves with field. This is not seen in oxygenated samples with similar metallic normal resistivities. As the peak resistivity may exceed the normal resistivity, it cannot arise from ordinary vortex-motion dissipation. We propose a model where the excess resistance results from nonrigid vortex motion coupling the out-of-plane dissipation to the in-plane resistance at temperatures where pinning effects are negligible.

PACS numbers: 74.60.Ge

The nature of the resistive transitions in magnetic fields and the role of vortex motion in causing dissipation in the layered cuprate superconductors have been lively questions with ramifications for both science and applications. Since a clear understanding of field-induced dissipation is of great importance, this subject has generated intense experimental and theoretical interest and controversy. Typically, with the field oriented in the  $c$  direction, perpendicular to the planar Cu-O layers, and the current in the  $a$ - $b$  direction along the planes, these materials exhibit a transition onset temperature that is not greatly affected by fields up to  $\sim 10$  T, followed by an anomalously broad transition region. These facts have generated various innovative models of vortex structure and dynamics which seek to explain the decay of resistance with temperature [1]. While there are many competing models for the  $a$ - $b$ -plane vortex dynamics [2], several reported data [3-5] on  $\text{Bi}_2\text{Sr}_2\text{CaCu}_2\text{O}_8$  and  $\text{Tl}_2\text{Ba}_2\text{CaCu}_2\text{O}_8$  display a prominent excess dissipation at high fields in the form of a resistive "knee" or a "hump" at temperatures between 50 and 80 K that, due to the intermediate temperature range involved, is difficult to explain with current models.

In this Letter we report the first observation of a field-induced resistive maximum that can exceed the extrapolated normal-state resistivity in the  $a$ - $b$ -plane transition of oxygen-reduced  $\text{Bi}_2\text{Sr}_2\text{CaCu}_2\text{O}_{8+\delta}$  single crystals. This occurs despite the metallic and relatively low normal resistivity  $\rho_n(T)$  in these samples. Because  $\rho_n(T)$  is metallic, this effect cannot be explained by conventional motion of vortices. We propose a simple model for the excess resistance, caused by motion of nonrigid vortex lines, that is independent of the details of the in-plane vortex motion and dissipation. This model can account for the present data and may apply to other layered superconducting systems as well. By comparing reduced crystals to oxygenated ones, where the resistance maximum does not develop at similar fields, we can gain insight into what material parameters affect the bending and interlayer coupling of vortex lines.

The single crystals of  $\text{Bi}_2\text{Sr}_2\text{CaCu}_2\text{O}_{8+\delta}$  were grown by a directional solidification process, and their oxygen contents were controlled by annealing in reducing or oxidizing atmospheres as described in detail in a previous article [6]. The reduced samples were characterized by a  $T_c$  of 92 K and the oxygenated samples by a  $T_c$  of 83 K, measured by both transport and magnetization. More detailed studies [6,7] of the oxidation-reduction reaction showed that it was reversible and did not affect the crystal microstructure. X-ray-diffraction patterns indicated homogeneous single-phase material with an instrumentally sharp linewidth. The crystals were cut into bars of trapezoidal cross section with typical dimensions 5 mm  $\times$  0.5 mm  $\times$  0.025 mm, cleaved, and then four Au contacts were evaporated down the sides in a linear configuration. The data were carefully checked to be independent of exact contact configuration. Freedom from random contact problems was tested by exchanging the roles of the current and voltage leads on several samples and confirming that the data were unaffected (inset of Fig. 1). The current was directed along the  $a$ - $b$  plane; both ac and dc biases were used with a current density of  $J \leq 50$  A/cm<sup>2</sup>, where the current-voltage relation was verified to be Ohmic in the temperature range concerned. The magnetic field was oriented in the  $c$  direction and varied from 0 to 10.5 T.

Figure 1 shows the resistivity versus temperature, in fields up to 10.5 T, of a sample annealed at 500 °C in a 0.1% H<sub>2</sub>/Ar-reducing atmosphere.  $\rho_n(T)$  is linear, metallic, and of moderately low resistivity, showing that, in the normal state,  $c$ -axis conduction is negligible. Superconducting fluctuations are evident above 90 K at all fields, indicating that the onset temperatures change little with field, consistent with this family of materials. The zero-field transition has no anomalies. Upon increasing field, however, a striking resistive peak evolves continuously with field between 55 and 80 K, developing from a knee below  $\sim 2$  T to a peak above 2 T, and exceeding  $\rho_n(T_c)$  around 6 T. These data strongly suggest that the

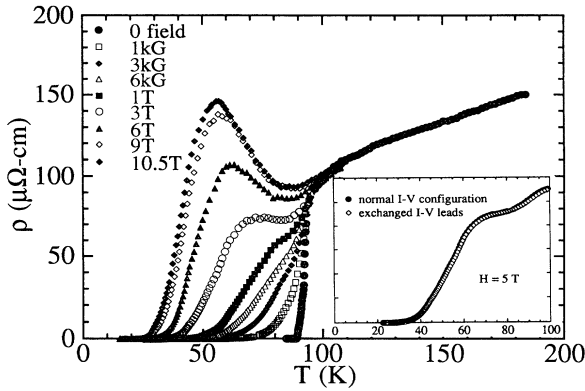


FIG. 1. *a-b*-plane resistive transitions in various perpendicular magnetic fields for a sample annealed in 0.1%  $H_2/Ar$ , showing the evolution of the resistance peak. Inset: Two sets of data on a similar sample with the roles of the current and voltage contacts exchanged, showing the independence of the data from possible contact problems.

development of knees in the same temperature range in the Refs. [3–5] are manifestations of the same phenomenon only with a larger characteristic field. In this temperature range the dc magnetization of these samples is reversible, indicating that pinning does not dominate the vortex dynamics here. All three such samples measured yielded similar results. Figure 2 shows, for comparison, a sample annealed at  $500^\circ C$  in 1 atm pure  $O_2$ .  $\rho_n(T)$  again is linear, metallic, and of similar magnitude to the reduced samples, but no peak develops up to 9 T. Three such samples confirmed this behavior. We remark that the presence or absence of resistive peaks bore no correlation with the magnitude of  $\rho_n$  above  $T_c$  or the  $T=0$  intercept extrapolated from high temperature.

This nonmonotonic, magnetic-field-dependent behavior of the transition is surprising, especially in view of the monotonically decreasing  $\rho_n(T)$ . Recently, Briceño, Crommie, and Zettl [4] have shown that when the current and field are both parallel to the  $c$  axis, a resistance maximum occurs, even at zero field, due to competition between the semiconducting  $c$ -axis normal resistivity and Josephson interplanar coupling. This is not expected to occur in the *a-b*-plane transition when a metallic  $\rho_n(T)$  is present. Because the behavior is associated with magnetic field in a relatively high-temperature regime, vortex motion will certainly be important. However, because  $\rho_n(T)$  decreases with  $T$ , whatever model is used for the *a-b*-plane vortex motion [2] cannot result in a vortex-induced resistance that exceeds  $\rho_n(T_c)$ . As emphasized by Briceño, Crommie, and Zettl [4], this is true in the Bardeen-Stephen model [8] even if  $\rho_n(T)$  is semiconducting.

We introduce here a new model, unique to weakly coupled layered superconductors, which proposes that motion of distorted vortices can produce an excess dissipation by coupling in  $c$ -axis current paths in addition to the *a-b*-

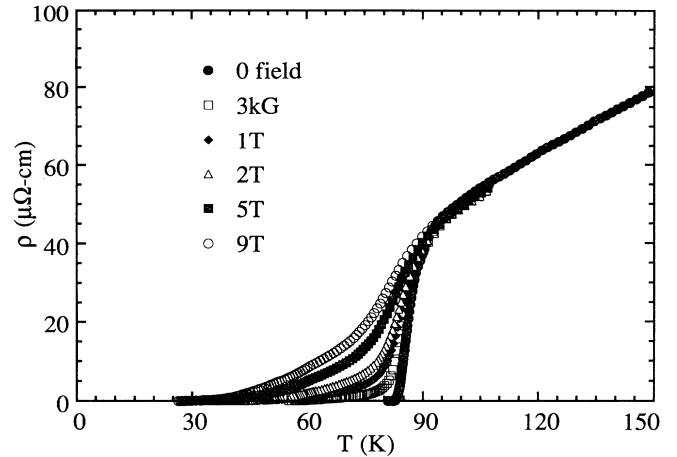


FIG. 2. *a-b*-plane resistive transitions in various perpendicular magnetic fields for a sample annealed in oxygen. No excess resistance appears up to 9 T.

plane resistance caused by vortex motion. This model accounts for at least the qualitative features of the data in Fig. 1. We assume that below  $T_c$  (onset) the layers can be thought of as Josephson coupled, and that this weak coupling allows distortions and nonrigid movement of vortex lines. It has been persuasively argued by many authors [9] that weak interlayer coupling will result in a small vortex-line tension and hence a significant probability that the vortex line is neither straight nor rigid. The problem is exacerbated by the presence of random pinning [10]. When the distorted vortex line moves, the time-dependent interlayer phase difference arising from the motion results in resistive interlayer current jumps, coupling in the larger  $c$ -axis dissipation to current flow nominally in the *a-b* plane.

Consider a vortex line which is primarily in the  $c$  direction but with a kink in the  $b$  direction, shown schematically in Fig. 3(a). The local vector potentials  $A_n(x, y, t)$  and  $A_{n+1}(x, y, t)$  in the  $n$  and  $n+1$  layers will then be unequal and will have some  $c$ -axis component, resulting in an interlayer local phase difference:

$$\gamma_{n,n+1}(x, y, t) = \frac{2\pi}{\Phi_0} d_c [A_{n+1}(x, y, t) - A_n(x, y, t)], \quad (1)$$

where  $d_c$  is the interlayer spacing. In the equilibrium case (i.e., no bias current) this phase difference will give rise to a supercurrent circulation with a  $c$ -axis component. This is just the screening current set up to shield the  $b$ -axis component of the field resulting from the bend in the vortex line [11]. If the vortex moves in response to a small applied current passed in the  $a$  direction, the local vector potentials will change with time, resulting in an interlayer voltage:

$$V_{n,n+1}(x, y) = \frac{\hbar}{2e} \frac{\partial \gamma_{n,n+1}}{\partial t} = \frac{\hbar}{e} \frac{\pi}{\Phi_0} d_c \left| \frac{\partial A_{n+1}}{\partial t} - \frac{\partial A_n}{\partial t} \right|. \quad (2)$$

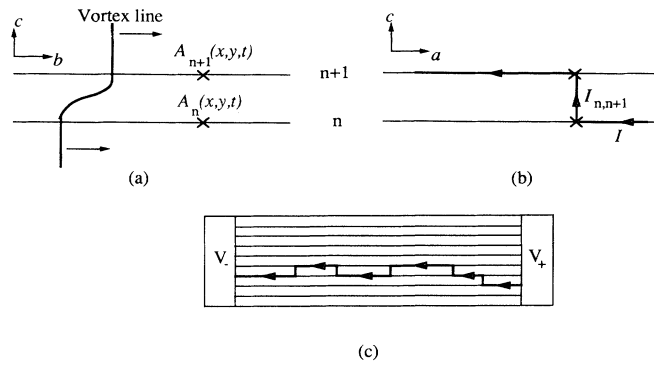


FIG. 3. Schematic representations of (a) a distorted vortex line and the local vector potentials, (b) the local interlayer current jump caused by motion of the distorted vortex line, and (c) an idealized current path between voltage electrodes. Inter-layer segments contribute resistance  $R_{\perp}$  independent of direction.

This voltage is a measure of the  $c$ -axis energy dissipation. If the vortex is a classical straight, rigid rod, by symmetry the time derivatives in (2) cancel and so no voltage develops. In the present case this voltage will cause some current to locally jump either from the  $n$  to the  $n+1$  layer [as shown schematically in Fig. 3(b)] or from the  $n+1$  to the  $n$  layer, depending on the bend direction of the vortex, with magnitude  $I_{n,n+1}(x,y) = V_{n,n+1}(x,y)/R_{\perp}$ ,  $R_{\perp}$  being the resistance in the  $c$  direction. Note that inter-layer current jumps in either direction both dissipate energy; hence, the absolute value is used in (2) so that the resulting voltages do not cancel (i.e., there is no energy-gain mechanism to give a voltage of opposite sign). Equation (2) gives the energy loss arising from one current jump due to motion of one vortex. Since all such jumps are dissipative, the total measured energy loss, in addition to the  $a$ - $b$  component, is just the sum of all such losses arising from all the vortices in the sample:

$$V(T,H) = I_{\text{bias}} R_{ab}(T,H) + \frac{R_{\perp}}{L^2} \sum_n \iint I_{n,n+1}(x,y) dx dy, \quad (3)$$

where  $I_{\text{bias}}$  is the set current bias and  $L^2$  is the planar area of the sample. Note that the excess dissipation due to vortex distortions is independent of whatever drives the in-plane vortex motion. Rewriting (3) in terms of resistance, we obtain

$$R(T,H) = \frac{V(T,H)}{I_{\text{bias}}} = R_{ab}(T,H) + \frac{I_{\perp}(T,H)}{I_{\text{bias}}} R_{\perp}(T), \quad (4)$$

where  $R(T,H)$  is the measured resistance and  $I_{\perp}(T,H)/I_{\text{bias}}$  is the total component of dissipative interlayer current.  $R_{\perp}(T)$  is the  $c$ -axis resistance obtained from data. Although (4) results from simply adding up energy

losses, one can picture it as a series-resistor network as shown in Fig. 3(c), where each interlayer segment yields a resistance  $R_{\perp}$ . The series, rather than parallel, path works because, just as in classical flux-flow resistance, the presence of moving vortices prevents the current from seeking an equilibrium path of least resistance, as emphasized by Tinkham [12].

All of the physics is encompassed in the function  $I_{\perp}(T,H)$  which, given a detailed model of the statics and dynamics of the vortices, is in principle easily calculated from (1) to (3). Although such knowledge of vortex behavior does not presently exist, some physical limits can nevertheless be deduced.

(i)  $I_{\perp}(T,H) \rightarrow 0$  as  $T \rightarrow T_c$  (onset) because the superconductivity is lost, so that the vortex is no longer quantized and the Josephson coupling vanishes.

(ii)  $I_{\perp}(T,H) \rightarrow 0$  as  $T \rightarrow 0$  because below some temperature the vortices are expected to either freeze or become pinned and not move in response to a small applied current. Furthermore, if the vortex distortion is thermally activated, there will be fewer line distortions and, hence, fewer current jumps at  $T \rightarrow 0$ .

(iii)  $I_{\perp}(T,H) \rightarrow 0$  for  $H < H_{c1}$ , since in the Meissner phase there are no vortices to drive the interlayer transitions.

(iv)  $I_{\perp}(T,H)$  is an increasing function of increasing  $H$  at given  $T$ . In low fields [ $(\Phi_0/H)^{1/2} > \lambda$ ],  $I_{\perp}(T,H)$  is expected to be linear with  $H$ , but modifications to this dependence at high field due to vortex-vortex correlations and inhomogeneity of field distribution are likely to be important. While such effects are difficult to estimate, the 9- and 10.5-T data of Fig. 1 suggest that  $I_{\perp}(T,H)$  saturates as  $H \rightarrow H_{c2}$ , indicating that competing effects may exist at high fields.

By (i) and (ii),  $I_{\perp}(T,H)$  must have a maximum between 0 and  $T_c$ , but because the physical reasons for vanishing at these limits are different,  $I_{\perp}(T,H)$  should not be symmetric about its maximum. Nevertheless, taking (iii) into account, for the purposes of simplicity of numerical computation, we take the functional form

$$I_{\perp}^{\text{sim}}(T,H) = aH \exp[-\sigma(T - T^*)^2], \quad (5)$$

bearing in mind that, although for practical purposes the Gaussian obeys the correct limits, it is used purely for convenience and is not physically justified. Some computed  $R(T,H)$  curves are shown in Fig. 4, taking data from an oxygenated sample for  $R_{ab}(T,H)$  and zero-field  $c$ -axis resistivity data [4,13] to generate  $R_{\perp}(T)$ . The important feature here is that the evolution of the resistive peak with field is clearly reproduced [14]. Where the simulation departs from the data in the temperature range  $T^* \leq T \leq T_c$  can be traced to the artificial symmetry of (5) about  $T^*$ . Experimentally, it appears that  $I_{\perp}(T,H)$  decays more slowly above  $T^*$  than below.

These simulations also argue against the possibility that the  $c$ -axis contribution is present in the normal state.

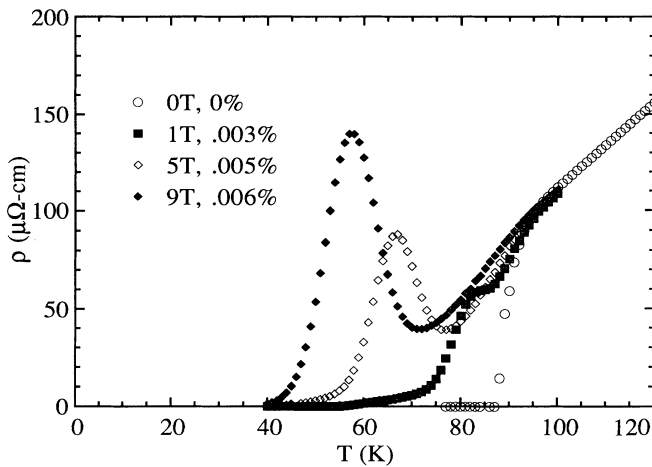


FIG. 4. Simulated  $\rho(T, H) = R(T, H) \times (\text{area}/\text{length})$  using Eq. (5) with  $\sigma^{-1} = 60$ , showing the evolution of a resistive peak. The percentages shown are the fitted magnitudes of  $I_{\perp}(T, H)/I_{\text{bias}}$ .  $R_{ab}(T, H)$  and  $R_{\perp}(T)$  contributions are obtained from measured data.

If in the normal state the same  $I_{\perp}/I_{\text{bias}}$  percentage necessary to generate a peak comparable to the data is present, simulations show that  $\rho_n(T)$  will be significantly larger in magnitude ( $\geq 500 \mu\Omega \text{ cm}$ ) than observed, nearly temperature independent, and that the fluctuation region will not be present due to the absence of fluctuations in the  $c$ -axis transition [4,13]. None of this agrees with the data of Fig. 1.

Within the context of this model, the correlation of the resistive peak with the oxygen content of the  $\text{Bi}_2\text{Sr}_2\text{CaCu}_2\text{O}_{8+\delta}$  samples implies that the material parameters governing the vortex-line tension is altered by oxygen doping. It is believed that the oxygen moves primarily into and out of the interplanar Bi-O layer, so that the presence of oxygen between Cu-O planes seems to increase the effective line tension for reasons that are currently being explored. X-ray-diffraction and Hall-effect measurements on these samples also show that the  $c$ -axis lattice constant shrinks slightly and the carrier density increases as the oxygen content is increased [6,7]. These effects may serve to decrease the effective anisotropy, resulting in a diminished probability of a kink developing in any given vortex line. As such, the characteristic field at which the excess resistance becomes discernible may be increased over the more anisotropic samples.

We thank L. Lombardo for help with magnetometer measurements and D. A. Huse for useful discussions. J.W.P.H. acknowledges partial support from the John and Fannie Hertz Foundation. Work at Stanford was

supported in part by the AFOSR Superconductivity Center and by the NSF Center for Materials Research.

(a) Present address: AT&T Bell Laboratories, Murray Hill, NJ 07974.

(b) Present address: IBM T. J. Watson Laboratory, Yorktown Heights, NY 10598.

- [1] See *Proceedings of the International Conference on  $M^2S$ -HTSC II, Stanford, California* [Physica (Amsterdam) **162-164C** (1989)], for an extensive summary.
- [2] See, for example, M. Tinkham, Phys. Rev. Lett. **61**, 1658 (1988); D. H. Kim *et al.*, Phys. Rev. B **42**, 6249 (1990); M. C. Marchetti and D. R. Nelson, Phys. Rev. B **42**, 9938 (1990); D. S. Fisher, M. P. A. Fisher, and D. A. Huse, Phys. Rev. B **43**, 103 (1991), and references therein.
- [3] T. T. M. Palstra *et al.*, Phys. Rev. Lett. **61**, 1662 (1988).
- [4] G. Briceño, M. F. Crommie, and A. Zettl, Phys. Rev. Lett. **66**, 2164 (1991).
- [5] K. Togano *et al.*, Jpn. J. Appl. Phys. **28**, L907 (1989); H. Mukaida *et al.*, Phys. Rev. B **42**, 2659 (1990).
- [6] D. B. Mitzi *et al.*, Phys. Rev. B **41**, 6564 (1990).
- [7] D. B. Mitzi, Ph.D. thesis, Stanford University, 1990 (unpublished).
- [8] J. Bardeen and M. J. Stephen, Phys. Rev. **140**, A1197 (1965).
- [9] D. R. Nelson and S. Seung, Phys. Rev. B **39**, 9153 (1989); S. Doniach, in *High Temperature Superconductivity Proceedings*, edited by K. S. Bedell, D. Coffey, D. E. Meltzer, D. Pines, and J. R. Schrieffer (Addison-Wesley, Redwood City, CA, 1989), p. 406; G. Deutscher and A. Kapitulnik, Physica (Amsterdam) **168A**, 338 (1990).
- [10] T. L. Hylton and M. R. Beasley, Phys. Rev. B **41**, 11669 (1990).
- [11] Note that, in the equilibrium case, there is no dissipation from the induced currents. Indeed, dc magnetization measurements on these samples show no anomalies at the relevant fields and temperatures of the resistive peaks. The excess dissipation is strictly a nonequilibrium phenomenon.
- [12] M. Tinkham, *Introduction to Superconductivity* (Krieger, New York, 1975), p. 165.
- [13] N. Hess, G. Deutscher, L. Lombardo, and A. Kapitulnik, in *Proceedings of the International Conference on Materials and Mechanisms of Superconductivity—High Temperature Superconductors III, Kanazawa, Japan* [Physica (Amsterdam) C (to be published)].
- [14] In order to fit the data, the fitted maximum  $T^*(H)$  must decrease with increasing  $H$ . This does not arise naturally from Eq. (5) because of the artificiality of the Gaussian. Physically, the inferred maximum in  $R(T, H)$  is expected to decrease in temperature with increasing field due to greater weight being given to the semiconducting  $R_{\perp}(T)$  of Eq. (4) in larger fields at any given temperature as discussed in point (iv) in the text.